7.6 USING WINDS FROM THE 4-D VARIATIONAL DOPPLER RADAR ANALYSIS SYSTEM (VDRAS) TO NOWCAST CONVECTION IN TAIWAN

Amanda R. S. Anderson*, James W. Wilson, Tracy J. Emerson, Zhuming Ying,
Juanzhen Sun, Rita D. Roberts
National Center for Atmospheric Research, Boulder, Colorado

1. INTRODUCTION

The complex terrain of Taiwan presents a difficult problem in nowcasting the initiation of convection in the country. The National Center for Atmospheric Research (NCAR) has been collaborating with the Taiwan Central Weather Bureau (CWB) to research heavy rainfall-producing convection on the island, specifically related to predicting initiation of such storms, and to transfer/tune the AutoNowCaster (ANC) system to aid in nowcasting this convection.

The ANC is an expert system that produces rapidly updating, one-hour nowcasts of thunderstorm initiation, growth, and decay (Mueller et al. 2003). The system ingests model data, surface observations, satellite, and radar data. These data are processed and run through a system of fuzzy logic equations and weights to produce one-hour interest field nowcasts that update approximately every five minutes. In addition to these data, forecaster input is an essential component of the system and is being tested as part of the Forecaster Over the Loop (FOTL) project (Roberts et al. 2005). In addition to the testing occurring in the United States, NCAR is refining and testing the ANC in Taiwan for the purpose of predicting heavy rainfall.

In the complex terrain of Taiwan, it would seem likely that wind direction and magnitude have a significant impact on the formation and location of convection and heavy rainfall (e.g., Chen and Chen 2003). As such, accurate wind analyses would be essential for systems such as the ANC to make useful nowcasts. To this end, the Variation Doppler Radar Analysis System (VDRAS; Sun and Crook 2001) is used within the ANC to provide predictors related to the wind field.

Initial observations with VDRAS winds over Taiwan showed that in synoptically forced, widespread rainfall situations, VDRAS has enough radar data to perform a representative analysis of the wind field, including some smaller-scale wind shifts that may impact where more intense storms form (Anderson et al. 2010). However, wind direction would be expected to play an especially important role in cases where the synoptic forcing is weak, and local forcings are the primary indication of where and when storms will initiate (e.g., Akaeda et al. 1995).

To best incorporate wind analyses into the ANC for nowcasting heavy rainfall-producing convection, VDRAS was run for 17 cases that occurred during the Southwest Monsoon Experiment/Terrain-influenced Monsoon Rain Experiment (SoWMEX/TiMREX; Jou et al. 2010), and the resulting wind fields compared to initiation locations.

Initial work focused on examining the overall domain for all case days as well as a closer analysis of two cases identified as having the highest quality input data, and consequently the most accurate VDRAS analyses (Anderson et al. 2011). No wind patterns were identified that directly corresponded with initiation location patterns, such as could be used as an ANC predictor field. However, areas of apparent upslope were identified. This paper discusses the results of continued work focused on the role of terrain in inducing upward motion, and how it may relate to initiation locations and ultimately how it may be incorporated into the ANC.

2. DATA

The SoWMEX/TiMREX field project was conducted jointly between the United States and Taiwan during the 2008 monsoon season in southwestern Taiwan (May-June). Many cases during this period involved the Mei-Yu front, which was a focus of the experiment (Chen 2004; Ciesielski et al. 2010), and past work has indicated that VDRAS performs well during such cases, where widespread rain provides ample radar velocity data for analysis (Anderson et al. 2010), and such analyses can be useful for detecting convective initiation (Sun et al. 2010).

**Corresponding author address:* Amanda R. S. Anderson, National Center for Atmospheric Research, P.O. Box 3000, Boulder, CO 80307;
email: aander@ucar.edu

Winds are expected to become especially important in cases of weak synoptic-scale forcing, where local circulations play a large role. To examine VDRAS's performance and utility for such cases, 17 days of weak synoptic-scale forcing were chosen from the SoWMEX/TiMREX dataset (see Anderson et al. 2011, Table 1).

VDRAS is a 4-D variational assimilation system that produces frequently updated (on the order of 10 minutes) analyses using Doppler radar, surface observations, and a mesoscale model background (Sun and Crook 2001). The mesoscale model is used to represent motion in the atmosphere, and then Doppler radar velocities are assimilated as well as surface observations to produce the VDRAS analysis. For this study, a Weather Research and Forecasting (WRF; Skamarock et al. 2005) simulation was used as the background field. Radar data was assimilated from two radars: the NCAR S-Pol polarimetric research radar (Keeler et al. 2000) that was set up for the field project and the operational Taiwanese RCCG radar at Chi-Gu (Fig. 1). Both radars operate at S-band. Surface data was also assimilated into VDRAS to produce the final wind fields.

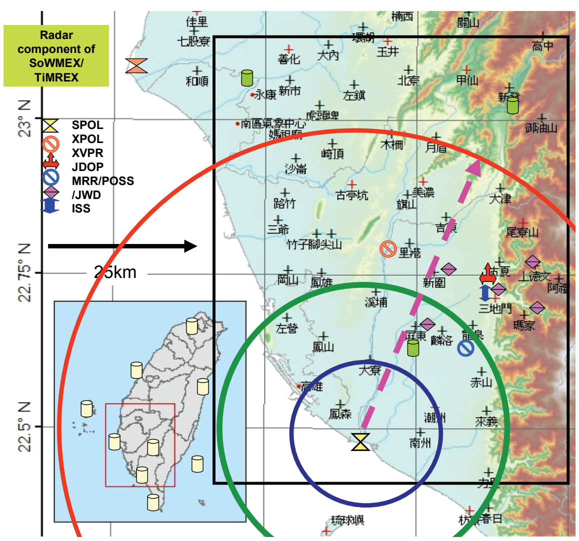

Fig. 1: Overview of surface observation network during SowMEX/TiMREX. S-Pol is located at the yellow hourglass and RCCG at the red hourglass. From Jou et al. (2010).

Initiation times and locations were identified on each of the days using S-Pol data and the Thunderstorm Identification, Tracking, Analysis, and Nowcasting (TITAN) algorithm (Dixon and Wiener 1993). TITAN drew a polygon around a cell provided it had reflectivity between 35 and 100 dBZ, was greater than 10 km^3 in echo volume, and persisted more than one radar scan. If the cell had actually reached 35 dBZ but was not detected by TITAN until later due to being too small in size, the earlier initiation time was used. Two cases with no initiation (21 June and 23 June) were included in the analysis to identify differences between weakly-forced days that did and did not produce convection.

To expand on the initial study, initiation locations were plotted on a terrain map to determine their location relative to the topography. Then, a simple model that calculates terrain-induced upward motion from an input wind direction and wind speed was run to assess the role wind, in conjunction with the complex terrain, had in initiation location.

3. USING VDRAS WINDS TO EXAMINE EFFECTS OF TERRAIN

To examine the idea that upslope flow may play a factor in initiation on these weak-forcing days, the pure upslope component of the VDRAS winds at the initiation locations was isolated. This was done in the method of Kodama and Barnes (1997). For this method, the direction of wind normal to the terrain is identified, and this is used to rotate the standard meteorological coordinate system such that the positive u-component of the wind is pure upslope, while the positive v-component is parallel to the slope. Because the terrain changes greatly, the normal component was calculated separately for each location by drawing a 7x7 grid point box around each initiation and calculating the slope through the center point. This slope was then used to rotate the coordinate system, and a time series of upslope wind direction was plotted for each initiation point. The change of upslope wind speed leading up to initiation was then subjectively analyzed, and results given in Table 1. For most cases, the upslope wind component changed little leading up to initiation. However, when looking purely at upslope versus downslope, twice as many cases had a positive upslope component in the time leading up to initiation. To examine the actual terrain features surrounding each initiation site in greater detail, each initiation location was plotted over a map of the terrain 0.2° latitude x 0.2° longitude surrounding the initiation point. These maps were then analyzed to determine the terrain feature over which the storm initiated. There were five categories: valley, slope, plain, summit,

Table 1: Number of cases by upslope component change and sign (positive for upslope, negative for downslope).

Upslope change	Increase	Steady	Decrease
	101	306	42
Upslope Direction	Positive	Negative	Zero
	288	144	17

and water. Examples of each of these categories are given in Fig. 2. The results of this analysis (Table 2) indicate that the vast majority of storms initiated in valleys or along slopes for these weak-forcing cases. This indicates that terrain, and possibly terrain-induced local circulations, plays a role in where storms form in weak synoptic forcing, despite the results from the upslope component analysis.

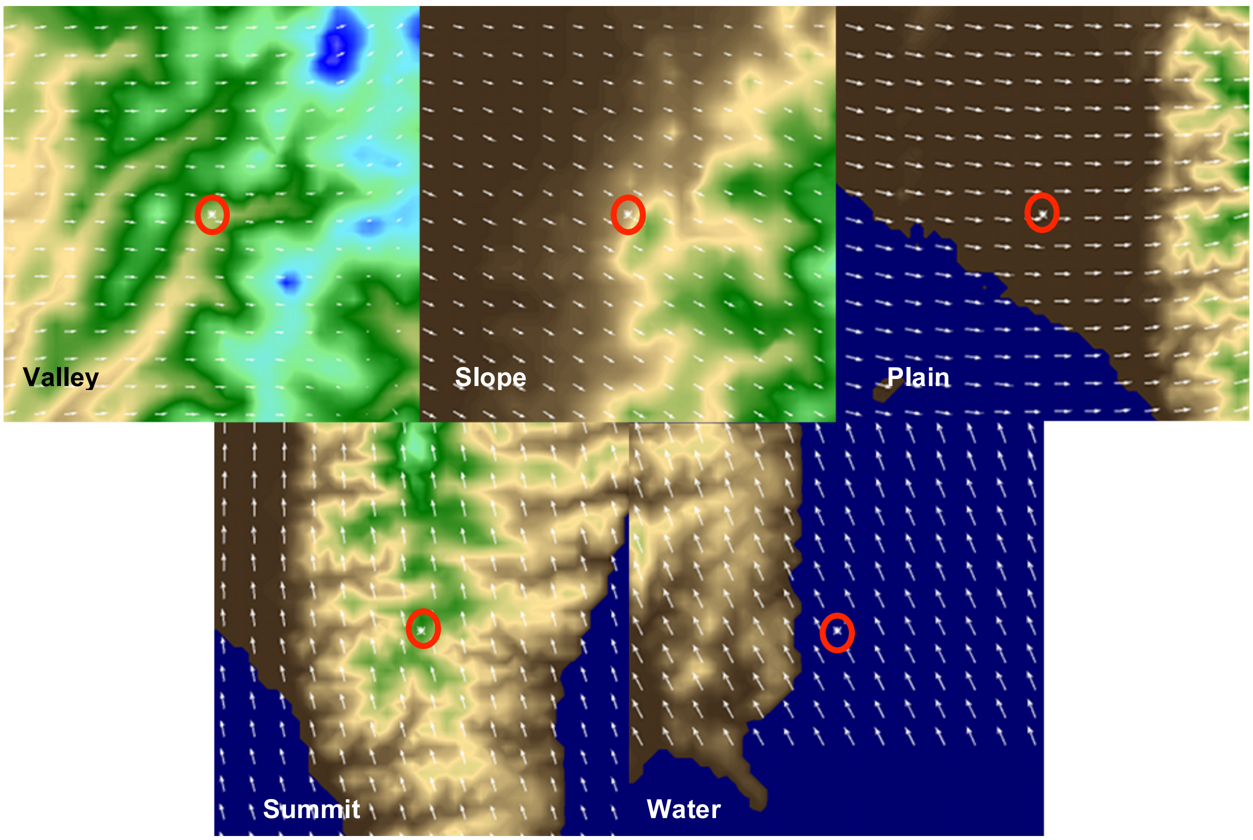

Fig. 2: Example of terrain features surrounding initiation points. Water is shaded navy blue, lowest terrain in the dark brown colors, increasing elevation through tan and green with dark blue the highest elevation. Initiations are marked with red circles.

Table 2: Terrain features of initiation locations. First row is number of initiations, second row is percentage of total initiations.

Valley	Slope	Plain	Summit	Water
238	208	29	7	3
49%	43%	6%	1%	1%

The prevalence of upslope flow and sloped terrain features in these small-scale analyses provided enough evidence of topography effects to continue to determine a way that the terrain-affected winds from VDRAS could be incorporated into the ANC's fuzzy logic. To this end, a program was used to compute the w component of the wind, forced by the terrain, from the horizontal VDRAS wind field, as described at the end of Section 2. The raw field was analyzed as well as both 9-point and 25-point terrain-smoothing fields.

First, updraft fields were computed for the two main cases examined in Anderson et al. (2011), 1 June and 7 June, using the overall wind directions of 230° and 180° respectively and a default wind of 10 m s^{-1}. In addition to presence of updraft or downdraft regions, the features of the terrain (e.g., Table 2) were also examined. Results are shown in Table 3. The specific terrain features mentioned in the table are illustrated in Fig. 2. Two additional features, the north-south oriented terrain of the southern Central Mountain Range (CMR) and a large valley in the northern part of the domain, were also included.

Table 3: Comparison of 1 June and 7 June initiation locations with surrounding terrain and output from terrain-induced upward flow model. Percentage of total initiations given in parentheses. Percentages do not add up to 100 because some initiations occurred in both types of terrain, e.g., forming along the slope of a valley. Perceived importance to total event given in last two columns.

Feature	1 June (26)	7 June (8)	1 June Importance	7 June Importance
Valley	18 (69%)	7 (88%)	Important	Very Important
Slope	21 (81%)	5 (63%)	Very Important	Important
Upward Motion	18 (69%)	2 (25%)	Important	Somewhat Important
Downward Motion	0 (0%)	4 (50%)	Not Important	Important
N-S Terrain	6 (23%)	0 (0%)	Somewhat Important	Not Important
Northern Valley	5 (19%)	0 (0%)	Somewhat Important	Not Important
Plain	1 (4%)	0 (0%)	Not Important	Not Important
Smoothing Conflicts	6 (23%)	3 (38%)	Somewhat Important	Somewhat Important
Unclassified	1 (4%)	0 (0%)	Not Important	Not Important

Over both cases, valley and slope features were important areas of convective initiation. For 1 June, the majority of initiation occurred in areas clearly defined as upward motion regions by the simple terrain-induced upward motion model. The north-south oriented terrain and northern valley areas were also important for 1 June. For the 7 June case, only 25% of initiations occurred in upward motion regions, and half occurred in areas designated as downward motion by the model. Because a prevailing wind of 180° and 10 m s^{-1} was the only wind used as input, it is possible that the actual updraft features were not properly captured, as winds further north and nearer the initiation areas had a stronger westerly component during this case than the winds in the southern part of the island, which were closer to the 180° used for the model. Additionally, it is important to note that multiple initiation locations for both cases had smoothing conflicts, meaning there was a difference between the w components of the wind (upward/downward) at the same location depending on the amount of smoothing.

The results for the 7 June case indicate that it may not be accurate enough from an initiation-prediction standpoint to classify an entire case with one wind direction. To account for this, the terrain-induced upward flow model was run for every degree of wind direction, 0°–359°. In order to bound the analysis, the default wind speed of 10 m s^{-1} was retained. The VDRAS wind direction at the closest time and point to the initiation was identified, then the proper upward motion value assigned to the initiation point. The results are presented in Fig. 3. Overall, the upward motion calculated by the model was mostly near 0 m s^{-1}, with a near-normal distribution of upward/downward motion around it. To test whether these results were negatively influenced by using a single, default wind speed, another test was run using model output from an input wind direction and wind speed that were both from VDRAS (Fig. 4). Typically the VDRAS wind speeds were less than 10 m s^{-1}, and this is reflected in the resulting weaker upward motions calculated from the model, all of which were between -0.5 and +0.5 m s^{-1}, essentially 0.

4. CONCLUSIONS

Given the results presented here, it is apparent that the terrain has some effects on initiation location. Over 90% of initiations on the weakly-forced days occurred in complex terrain. However, it is difficult to diagnose exactly what these effects are. It is possible that they are occurring at a scale too small to be resolved by

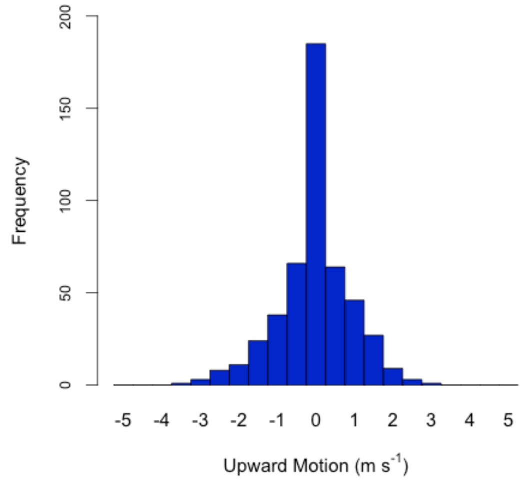

Fig. 3: Histogram of upward motion values calculated by the terrain-influenced upward motion model at each initiation location at the time of initiation. Input wind direction was taken from VDRAS analyses, input wind speed was 10 m s^{-1}.

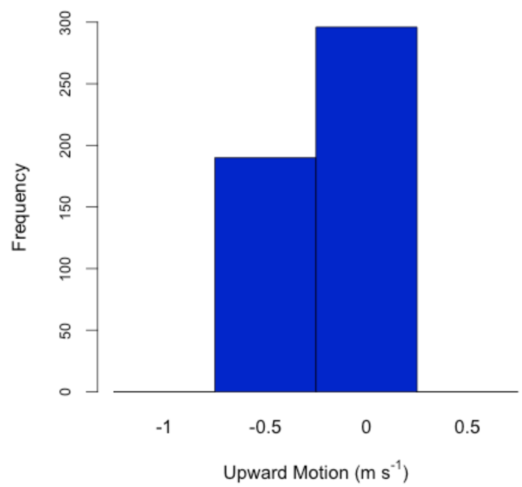

Fig. 4: Same as Fig. 3, but with input wind speed from VDRAS analyses.

VDRAS. They also may not be related to wind direction/speed at all, but rather thermodynamic effects, such as anabatic flow produced by unequal heating of the terrain.

From this work, it appears that at this point, when tuning the ANC system for Taiwan, fields other than wind direction and speed should be the focus on undisturbed days. An emphasis will be put on examining thermodynamic effects. VDRAS analyses could still be very useful in this regard, including the VDRAS temperature perturbation field. Other fields will also be considered, such as the hourly climatology presented in Lin et al. (2011), which reflects the general preferred areas of initiation on days with weak synoptic forcing.

5. REFERENCES

Akaeda, K., J. Reisner, and D. Parsons, 1995: The role of mesoscale and topographically induced circulations initiating a flash flood observed during the TAMEX project. Mon. Wea. Rev., 123, 1720–1739.

Anderson, A.R.S., J. Sun, R. Roberts, W-C. Lee, 2010: A comparison of SoWMEX/TiMREX wind observations with WRF and VDRAS 3-D wind fields on 31 May 2008. *Extended Abstracts, 3rd SoWMEX/TiMREX Science Workshop*, Taipei, Taiwan, Taiwan Weather Research Program, 4.2.

Anderson, A. R. S., J. W. Wilson, T. Emerson, Z. Ying, J. Sun, R. D. Roberts, 2011: Using winds from the 4-D Variational Doppler Radar Analysis System (VDRAS) to nowcast convection in Taiwan. *35th Conf. on Radar Meteorology*, Pittsburgh, PA, Amer. Meteor. Soc., 19A.4.

Chen, C.-S., Y.-L. Chen, 2003: The Rainfall Characteristics of Taiwan. *Mon. Wea. Rev.*, **131**, 1323–1341.

Chen, G.T.J., 2004: Research on the phenomena of Meiyu during the past quarter century: An overview. *East Asian Monsoon*, C. P. Chang, Ed., Series for Meteorology of East Asia, Vol. 2, World Scientific, 357–403.

Ciesielski, P.E., and Coauthors, 2010: Quality-Controlled Upper-Air Sounding Dataset for TiMREX/SoWMEX: Development and Corrections. *J. Atmos. Oceanic Technol.*, **27**, 1802–1821.

Dixon, M., and G. Wiener, 1993: TITAN: Thunderstorm identification, tracking, analysis, and nowcasting—A radar-based methodology. *J. Atmos. Oceanic Technol.*, **10**, 785–797.

Jou, B.J.-D., W.-C. Lee, and R.H. Johnson, 2010: An overview of SoWMEX/TiMREX. *Selected Papers of the Fourth International Monsoon Workshop*, C.P. Chang, Ed., World Scientific, 1–16.

Keeler, R.J., J. Lutz, and J. Vivekanandan, 2000: S-POL: NCAR's polarimetric Doppler research radar. Preprints, *IGARSS-2000*, Honolulu, HI, IEEE, 1570–1573.

Kodoma, K., and G. M. Barnes, 1997: Heavy rain events over the south-facing slopes of Hawaii: Attendant conditions. *Wea. Forecasting*, **12**, 347–367.

Lin, P.-F., P.-L. Chang, B. J.-D. Jou, J. W. Wilson, R. D. Roberts, 2011: Warm season afternoon thunderstorm characteristics under weak synoptic-scale forcing over Taiwan Island. *Wea. Forecasting*, **26**, 44–60.

Mueller, C., T. Saxen, R. Roberts, J. Wilson, T. Betancourt, S. Dettling, N. Oien, J. Yee, 2003: NCAR Auto-Nowcast System. *Wea. Forecasting*, **18**, 545–561.

Roberts, R., S. Fano, W. Bunting, T. Saxen, E. Nelson, C. Mueller, D. Megenhardt, D. Albo, S. Dettling, A. Crook, N. Oien, H. Cai, K. Johnston, S. Smith, M. Ba, and T. Amis, 2005: The NWS/NCAR Man In The Loop (MITL) Nowcasting Demonstration: Forecaster Input into a Thunderstorm Nowcasting System. *Proc. WWRP Symp. Nowcasting & Very Short Range Forecasting*, Toulouse, France, 5-9 September, 7.26.

Skamarock, W.C., J.B. Klemp, J. Dudhia, D.O. Gill, D.M. Barker, W. Wang, and J.G. Power, 2005: A description of the advanced research WRF version 2. NCAR Tech. Note TN-468+STR, 88 pp.

Sun, J., N.A. Crook, 2001: Real Time Low-Level Wind and Temperature Analysis Using Single WSR-88D Data. *Wea. Forecasting*, **16**, 117–132.

Sun, J., M. Chen, Y. Wang, 2010: A frequent-updating analysis system based on radar, surface, and mesoscale model data for the Beijing 2008 Forecast Demonstration Project. *Wea. Forecasting*, **25**, 1715–1735.